Development 133, 3745-3754 (2006) doi:10.1242/dev.02544

Depletion of the co-chaperone CDC-37 reveals two modes of PAR-6 cortical association in *C. elegans* embryos

Melissa Beers and Kenneth Kemphues*

PAR proteins play roles in the establishment and maintenance of polarity in many different cell types in metazoans. In *C. elegans,* polarity established in the one-cell embryo determines the anteroposterior axis of the developing animal and is essential to set the identities of the early blastomeres. PAR-1 and PAR-2 colocalize at the posterior cortex of the embryo. PAR-3, PAR-6 and PKC-3 (aPKC) colocalize at the anterior cortex of the embryo. A process of mutual exclusion maintains the anterior and posterior protein domains. We present results indicating that a homolog of the Hsp90 co-chaperone Cdc37 plays a role in dynamic interactions among the PAR proteins. We show that CDC-37 is required for the establishment phase of embryonic polarity; that CDC-37 reduction allows PAR-3-independent cortical accumulation of PAR-6 and PKC-3; and that CDC-37 is required for the mutual exclusion of the anterior and posterior group PAR proteins. Our results indicate that CDC-37 acts in part by maintaining PKC-3 levels and in part by influencing the activity or levels of other client proteins. Loss of the activities of these client proteins reveals that there are two sites for PAR-6 cortical association, one dependent on CDC-42 and not associated with PAR-3, and the other independent of CDC-42 and co-localizing with PAR-3. We propose that, in wild-type embryos, CDC-37-mediated inhibition of the CDC-42-dependent binding site and PAR-3-mediated release of this inhibition provide a key mechanism for the anterior accumulation of PAR-6.

KEY WORDS: Embryo, Polarity, Protein stability, CDC-42, PAR proteins

INTRODUCTION

Asymmetric cell division is a fundamental mechanism for generating cell diversity. The first division of the *C. elegans* zygote provides a unique opportunity to study the effects of polarity on the ability of a cell to divide asymmetrically into daughters with different fates. The par genes (partitioning defective) are key regulators of polarity in the early embryo (Kemphues et al., 1988). The PAR proteins are conserved widely in animals and play roles in such diverse cellular functions as asymmetric cell division, apicobasal polarity in epithelial cells, oriented cell migration, neuronal axis specification and tight junction formation (Nishimura et al., 2004; Ohno, 2001; Wiggin et al., 2005).

Considerable progress has been made in understanding events leading up to the first asymmetric division of *C. elegans*. After fertilization, the egg completes the meiotic divisions and produces egg coverings. Upon completion of meiosis, the zygotic surface begins to ruffle, the result of local cortical contractions. At the same time, the anterior PAR proteins (PAR-3, PAR-6 and PKC-3) appear uniformly at the cell periphery. Initially, the contractions are uniformly distributed over the surface, but shortly after the sperm pronucleus decondenses, the sperm centrosome signals to the cortex, leading to a local cessation of cortical ruffling and initiation of a cortical flow away from the posterior (Cheeks et al., 2004; Cowan and Hyman, 2004; Munro et al., 2004). The anterior PAR proteins move with the flow toward the anterior, clearing them from the posterior, and PAR-1 and PAR-2 proteins are recruited from the cytoplasm to the smooth cortex in the posterior. Flow depends upon the activities of the PAR proteins (Cheeks et al., 2004; Munro et al., 2004). Mutations in the anterior PAR proteins allow an initial smoothing of the posterior cortex, but either block or greatly attenuate the flow into the anterior (Cheeks et al., 2004; Kirby et al., 1990; Munro et al., 2004). After the establishment phase, PAR-2 protein mediates the maintenance of asymmetry (Cuenca et al., 2003), in part by inhibiting a posterior-directed flow of cortical cytoplasm (Munro et al., 2004), and in part by antagonizing its own removal from the cortex by PKC-3 phosphorylation (Hao et al., 2006).

The establishment and maintenance of stable polar PAR domains is based on the principle of mutual exclusion. In the absence of the anterior PAR proteins, PAR-1 and PAR-2 are not restricted to the posterior, and, in the absence of PAR-2, the anterior proteins, as already described, are not stably restricted to the anterior (Boyd et al., 1996; Cuenca et al., 2003; Etemad-Moghadam et al., 1995; Tabuse et al., 1998; Watts et al., 1996). The mutual exclusion of anterior and posterior PAR proteins depends upon the 14-3-3 family member PAR-5 (Morton et al., 2002).

Cortical localization of the anterior PAR proteins is dependent upon the activities of all three proteins: PAR-3, PAR-6 and PKC-3 (Hung and Kemphues, 1999; Tabuse et al., 1998; Watts et al., 1996). In *par-3* mutants, neither PAR-6 nor PKC-3 protein is detectable at the cell cortex. Similarly, in *par-6* mutants, PKC-3 is not detectable at the cortex, and in *pkc-3(RNAi)* embryos PAR-6 is absent. However, in *par-6* mutant and *pkc-3(RNAi)* embryos, PAR-3 accumulates weakly and somewhat asymmetrically at the cortex early in the cell cycle, but is undetectable after metaphase of mitosis. Cortical localization of the anterior PAR proteins also depends on a conserved interaction of PAR-6 with CDC-42, a Rho-family GTPase (Gotta et al., 2001; Kay and Hunter, 2001) (D. Aceto, M.B. and K.K., unpublished).

To find other proteins with possible roles in establishing polarity in *C. elegans*, we identified homologs of a set of human proteins that co-purified with PAR proteins (Brajenovic et al., 2004) and tested them by RNA interference (RNAi). RNAi knockdown of one of them, W08F4.8, a homolog of human CDC37, caused a PAR-like

Department of Molecular Biology and Genetics, 101 Biotechnology Building, Cornell University, Ithaca, NY 14853, USA.

*Author for correspondence (e-mail: kjk1@cornell.edu)

Accepted 20 July 2006

phenotype. Concurrent with our analysis, a genome-wide RNAi screen identified this same gene as one of a small number of genes whose knockdown results in PAR-like early cleavages (Sonnichsen et al., 2005). In addition, Gunsalus and colleagues reported the distribution of GFP::CDC-37 in the early embryo (Gunsalus et al., 2005).

CDC37 was initially identified by a temperature-sensitive mutation defective in the cell cycle at Start in G1 in *Saccharomyces cerevisiae* (Reed, 1980). Subsequent analysis revealed that Cdc37p acts by maintaining the cyclin-dependent kinase Cdc28p in a state that is competent to associate with G1 and mitotic cyclins (Gerber et al., 1995). Vertebrate Cdc37 homologs have been identified in a number of studies as ~50 kDa proteins that associate with Hsp90 and a variety of other proteins, particularly kinases (Hunter and Poon, 1997). The prevailing view is that Cdc37 functions as a co-chaperone of Hsp90, interacting with protein kinases to regulate their activity, either by enabling them to fold correctly for proper activation or by preventing them from being degraded (Hunter and Poon, 1997). Among the many kinases regulated by Cdc37 and Hsp90 are Raf1 (Grammatikakis et al., 1999; Perdew et al., 1997; Silverstein et al., 1998; Stancato et al., 1993), Cdk4 (Dai et al., 1996; Stepanova et al., 1996), Akt (Basso et al., 2002) and Lkb1, a homolog of *C. elegans* PAR-4 (Boudeau et al., 2003; Nony et al., 2003). However, evidence is accumulating that Cdc37 can act independently of Hsp90 and has a wider range of client proteins than has previously been appreciated (MacLean and Picard, 2003).

In this paper, we report that reduction of CDC-37 in the *C. elegans* early embryo alters the dynamic interactions among the PAR proteins, leading to Par-like embryonic phenotypes. Our analysis of the CDC-37 phenotype has provided insight into the mechanisms of anterior PAR protein accumulation at the cortex.

MATERIALS AND METHODS

Strains used

Nematodes were cultured under standard conditions (Brenner, 1974). The Bristol N2 strain was used as wild type. Strains used for this analysis were KK0818, *par-6(zu222) unc-101(m1)/hIn1 [unc-54(h1040)]I;* KK0653, *par-3(it71) unc-32(e0189)/qC1;* JH1448, *axEx1125 [pKR2.04, Ppie-1::GFP::MEX-5, pRF4, N2 genomic]* (Cuenca et al., 2003); SS629, *[pie-1::gfp::pgl-1, unc-119(+)]* (Cheeks et al., 2004); KK0881, *itIs160 [Ppie-1::GFP::PAR-6 unc-119(+)]; unc-119(ed3);* JJ1473, *zuIs45 [Pnmy-2::NMY-2::GFP unc-119(+)]; unc-119(ed3)* (Nance et al., 2003); KK0911, *itIs161 [Ppar-3::PAR-3 S863A::GFP unc-119(+)]; unc-119(ed3)]* (B. Li and K.K., unpublished). The PAR-3::GFP protein in KK0911 carries an alanine substitution in the PKC-3 phosphorylation site of PAR-3 (Serine 863). PAR-3 S863A::GFP rescues *par-3(it71)* and gives a stronger cortical signal than does wild-type PAR-3::GFP.

RNA interference

For some experiments dsRNA was injected into the gonad arms of the worms (Fire et al., 1998). In this case, dsRNA was made in vitro from L4440 plasmids (Timmons and Fire, 1998) containing the gene of interest, using the RiboMAX kit (Promega). In other experiments, the L4440 plasmids containing the gene of interest were induced with IPTG in HT115(DE3) bacteria to produce dsRNA, and the bacteria were fed directly to worms to produce the RNAi effect (Timmons et al., 2001). For most RNAi studies, treated worms were incubated at 25°C for at least 18 hours before either antibody staining or time-lapse microscopy. For *cdc-42(RNAi)* studies, injected worms were incubated at 20°C for 8 hours, then 25°C for at least 16 hours before analysis. The efficiency of each RNAi experiment was determined by assessing the number of dead embryos laid by a subset of treated worms. Because of variable effectiveness of RNAi in *C. elegans*, comparisons between the results of different experiments are only reliable where the penetrance of each experiment is high.

Imaging

Observations of live embryos with either DIC or fluorescence microscopy were made on a Leica DM RA2 microscope with a 63× or 100× Leica HCX PL APO oil emersion lens and Hamamatsu ORCA-ER digital camera. Digital images were captured using Openlab software (Improvision). All embryos were imaged at 22°C immersed in egg buffer (118 mM NaCl, 40 mM KCl, 3.4 mM $CaCl_2$, 3.4 mM $MgCl_2$, 5 mM Hepes, pH 7.4) on agar pads. The center of the embryo was chosen as the focal plane for the live observations. For cortical images, we focused at the cortex of partially flattened fixed embryos. We adjusted each image in PhotoShop, to remove background signal, by bringing the posterior cortical signal to zero. To count puncta, we sampled two similar-sized, non-overlapping windows from the center of the anterior cortex by laying an acetate sheet sequentially over the grayscale images of each fluorochrome and marking the positive puncta. We took the average of two samples for each embryo. Egg length was measured using Openlab software. Two-cell blastomere sizes were compared by measuring the length along the long axis of the embryo of AB and P1 in control and *cdc-37(RNAi)* embryos. Confocal images were collected on the Leica TCS SP2 system with the Leica DMRE-7 microscope and an HCX PL APO 63× oil immersion lens. Images were processed using the Leica Confocal SP2 software program and Adobe PhotoShop.

Immunohistochemistry

Immunostaining for PAR-2, PAR-3, PAR-6, PKC-3 and GFP was performed using a standard methanol fixation (Guo and Kemphues, 1995). Antibodies used were: anti-PAR-2 rabbit polyclonal (Boyd et al., 1996), 1:3; anti-PAR-3 mouse monoclonal (Nance et al., 2003), 1:75; anti-PAR-6 rabbit polyclonal (Hung and Kemphues, 1999), 1:15; anti-PKC-3 rat polyclonal (Hung and Kemphues, 1999), 1:10; and anti-GFP goat polyclonal (Rockland Immunochemicals), 1:3000. Slides were incubated with primary antibodies for 12-18 hours at 4°C. Slides were then washed three times in PBS, 0.5% Tween 20. All secondary antibodies were from Jackson Immunochemicals: goat anti-rabbit FITC, 1:200; goat anti-mouse Cy3, 1:250; donkey anti-rat Cy3, 1:400; donkey anti-goat FITC, 1:100. Embryos were treated with secondary antibodies for 3 hours at 37°C. Slides were washed as before and then covered with VectaShield (Vector Laboratories).

GFP::CDC-37 transgenic animals

We created a vector for expressing GFP::CDC-37 by inserting *cdc-37* cDNA (W08F4.8a, 1113 nucleotides, amplified from the Gibco Proquest Library) into the pJunc vector, a derivative of pMW1.03, constructed by Aaron Schetter (Gunsalus et al., 2005), which contains a 5.7 kb genomic fragment of *unc-119* (pPDMM016) (Maduro and Pilgrim, 1995) and a *par-2* coding sequence fused to GFP and driven by the *pie-1* promoter (Wallenfang and Seydoux, 2000). The *par-2* gene was removed from the vector by *Spe*1 cleavage and *cdc-37* cDNA was inserted into the same site. Low-copy integrated lines expressing GFP::CDC-37 in the germline were identified among *unc-119(ed3)* worms following microparticle bombardment (Praitis et al., 2001).

Testing for rescue of *cdc-37(RNAi)* by GFP::CDC-37

To test for rescue, worms carrying the GFP::CDC-37 transgene were injected with dsRNA specific to the first 160 nucleotides of the endogenous *cdc-37* 3′UTR. dsRNA specific to the 3′UTR of a gene is an effective RNAi trigger (Parrish et al., 2000). Progeny of the injected worms were assayed for lethality 48 hours after injection. Eighty-five to 100% of embryos from 20 wild-type worms were dead compared with 32-50% of embryos from 28 GFP::CDC-37-expressing worms.

Western blots

Populations of control or RNAi worms were collected from feeding plates 20 hours after feeding began; adults were bleached to obtain early embryos; and embryos were lysed in SDS sample buffer. Samples were analyzed by Bradford Assay (Bradford, 1976) to determine total protein present in each sample. Equal amounts of total protein were loaded onto an 8% SDS PAGE gel. The proteins were then transferred to nitrocellulose membrane for western blotting (Burnette, 1981) and stained with the MemCode Reversible Membrane Staining Kit (Pierce) to verify equal loading of samples. All primary antibodies were diluted 1:1000 in 1×TBST with 0.5% milk and

incubated overnight at 4°C. Appropriate HRP-conjugated secondary antibodies (Jackson ImmunoResearch) were diluted 1:5000 in 1×TBST with milk, incubated for one hour at 22°C, then washed with TBST three times for a total of 30 minutes. Bands were visualized using a chemiluminescence detection reagent (Amersham Biosciences).

Rescue of the *S. cerevisiae cdc37-34(ts)* mutant by yeast *CDC37* or *C. elegans cdc-37*

The wild-type *S. cerevisiae GAL1/10* promoter was cloned into the pRS416 (CEN) URA3 plasmid (New England BioLabs). Wild-type yeast *CDC37* or *C. elegans cdc-37* (W08F4.8) cDNA was cloned in frame behind the promoter. These constructs were transformed into the yeast strains DP007 (*cdc37-34ts*) or RMY326 (control; kindly provided by D. Picard, Geneva University, Switzerland). Yeast were assayed for growth on galactose media at 25, 30, 35 and 37°C to test for rescue. In the absence of an antibody specific to CDC-37, we cannot rule out the possibility that our negative result was due to low expression of the worm protein.

RESULTS

cdc-37(RNAi) embryos exhibit polarity defects

In a study to identify proteins that interact with the mammalian Par proteins, Cdc37 co-purified in complexes with both aPKC and LKB1 (Brajenovic et al., 2004). On the basis of this result, we sought to test Cdc37 homologs for roles in polarity establishment in *C. elegans*. Of the three potential Cdc37 homologs identified by sequence similarity, only one, W08F4.8, was predicted to encode a protein similar in overall size and domain structure to the *H. sapiens* CDC37 protein (see Fig. S1 in the supplementary material). W08F4.8 protein was found to interact with the Hsp90 family member DAF-21 in a yeast two-hybrid assay (Li et al., 2004).

In spite of sequence similarity to CDC37 and conservation of HSP-90 binding, we found that W08F4.8 cDNA expressed under the control of the yeast *GAL1/10* promoter was unable to complement a temperature-sensitive *cdc37* yeast mutation. Even though *C. elegans* W08F4.8 failed this test for orthology with yeast *CDC37*, it is the *C. elegans* gene most similar in sequence to yeast, fruit fly and mammalian Cdc37 proteins. Therefore we refer to the gene as *cdc-37*.

To test whether CDC-37 has a role in embryonic polarity in *C. elegans*, we depleted the message from early embryos by using RNAi. Wild-type worms injected with dsRNA specific to *cdc-37* show increasing levels of embryo lethality: 30% at 0-17 hours versus >80% 18-24 hours post-injection. Embryos collected at this time show an approximately 80% reduction in steady-state GFP::CDC-37 levels (see Fig. S2 in the supplementary material). All embryos used for phenotypical analysis were dissected during this latter interval. Injected worms become sterile approximately 24 hours after injection. Sterile animals have sperm in the spermatheca as determined by DAPI staining, and developing oocytes are present; however, oocytes accumulate behind the spermatheca, suggesting a failure in egg maturation or ovulation (McCarter et al., 1999). Approximately 18% of the worms that escape embryonic lethality show a protruding vulva phenotype. Other less frequently observed post-embryonic phenotypes include larval arrest and tail rupture.

The affected embryos from *cdc-37(RNAi)* worms exhibit defects consistent with a loss of embryonic polarity (Fig. 1). The extent of cortical ruffling in *cdc-37(RNAi)* embryos varies from almost normal to barely detectable (Fig. 1F,G). The position of the pseudocleavage furrow in *cdc-37(RNAi)* embryos does not differ from that of controls (n=9 wild type and 11 *cdc-37(RNAi)*; P=0.24). However, the pseudocleavage invaginations in *cdc-37(RNAi)* embryos are shallow (37.9±13.2 μm versus 47.4±5.1 μm in wild type, P=0.012), tend to be unilateral (Fig. 2G; 6/11 embryos), and

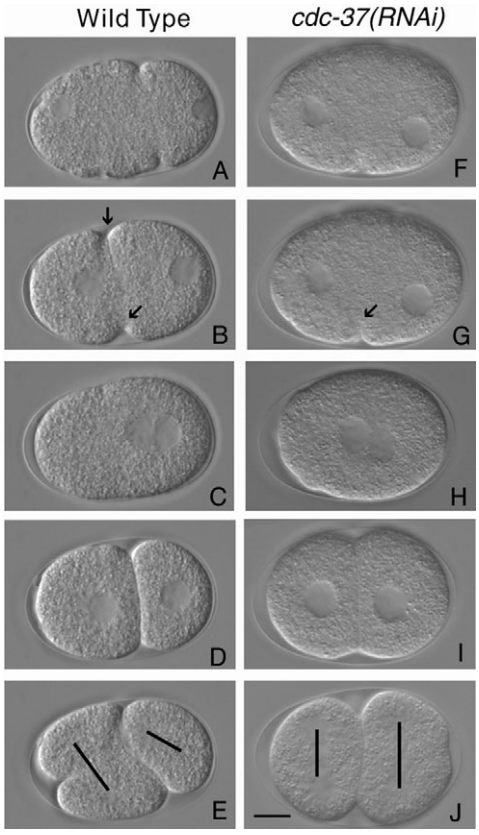

Fig. 1. Depletion of CDC-37 causes polarity defects. Anterior is to the left for all embryos in all figures. (**A-J**) Timed sequences of differential interference contrast photomicrographs of a wild-type embryo (A-E) and a *cdc-37(RNAi)* embryo (F-J) dissected 20 hours after dsRNA injection. The arrows in B,G mark the pseudocleavage furrow. Note the central meeting of the two pronuclei (H). Note the nearly equal size of the two blastomeres (I) and the abnormal spindle orientation (bars, J). Scale bar: ~10 μM.

are short lived (113±22 seconds, n=11, versus 191±56 seconds in wild type, n=11; P=0.0003). In *cdc-37(RNAi)* embryos, the two pronuclei meet more centrally (Fig. 1C,H; 56±8% egg length versus 70±3% egg length in wild type; n=14; P<0.0001) and the first cleavage is more equal (Fig. 1I; AB, the anterior two-cell stage blastomore, occupies 52±4% of total egg length, n=39, versus 58±2% in wild type, n=17; P<0.0001). The second cleavage is more synchronous after *cdc-37(RNAi)* (Fig. 1J) and is slightly slower than wild type. In *cdc-37(RNAi)* embryos, the period between nuclear envelope breakdown (NEB) in the zygote, P0, to NEB in its daughter cells AB and P1 was 1070±82 seconds, whereas the time between NEB in P0 and AB in wild type was 859±49 seconds (P<0.0001), and the time between NEB in P0 and P1 was 966±58.5 (P=0.0018; n=9, wild type; n=11, *cdc-37(RNAi)*). In contrast to the reproducible orthogonal spindle orientations of wild-type two cell embryos (n=11), *cdc-37(RNAi)* embryos display a variety of spindle orientations, with 85% exhibiting phenotypes different from wild type (Fig. 1J; n=39): 56% of the two-cell embryos divide with both spindles transverse to the long axis.

We also examined molecular markers of embryonic polarity, GFP::MEX-5 (Cuenca et al., 2003; Schubert et al., 2000) and P granules using GFP::PGL-1 (Cheeks et al., 2004; Strome and Wood, 1982; Strome and Wood, 1983). We found that asymmetry of both

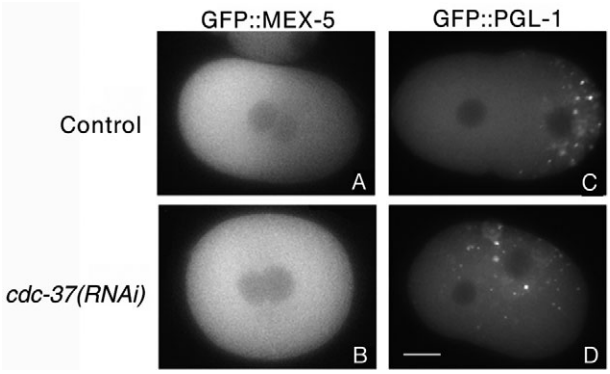

Fig. 2. MEX-5 protein and P-granule distributions are disrupted in *cdc-37(RNAi)* embryos. (**A**) GFP::MEX-5 in control embryos. (**B**) MEX-5::GFP in *cdc-37(RNAi)* embryos. (**C**) GFP::PGL-1 in control embryos. (**D**) GFP::PGL-1 in *cdc-37(RNAi)* embryos. All images are from live embryos. Scale bar: 10 μm.

markers is dependent upon CDC-37 (Fig. 2; for GFP::MEX-5, asymmetry was normal in 8/8 wild-type versus 1/10 *cdc-37(RNAi)* embryos; for GFP::PGL-1, asymmetry was normal in 12/12 wild-type versus 6/16 *cdc-37(RNAi)* embryos).

The PAR proteins are mislocalized in *cdc-37(RNAi)* embryos

Many of the phenotypes described above are also exhibited by mutations in the *par* genes (Kemphues et al., 1988; Kirby et al., 1990; Morton et al., 2002; Tabuse et al., 1998; Watts et al., 1996). We tested whether depletion of CDC-37 alters the distributions of the PAR proteins. Five PAR proteins have a highly reproducible asymmetry in the developing embryo. PAR-3, PAR-6 and the atypical protein kinase C PKC-3 colocalize to the anterior cortex of the one-cell embryo (Etemad-Moghadam et al., 1995; Hung and Kemphues, 1999; Tabuse et al., 1998), and PAR-1 and PAR-2 co-localize to the posterior cortex of the embryo (Boyd et al., 1996; Guo and Kemphues, 1995). We found that the distribution of both sets of proteins is dramatically altered by depletion of CDC-37.

In contrast to control embryos (Fig. 3A-C, *n*=32; Fig. 4, column 3, *n*=13) PAR-1, PAR-2, PAR-6 and PKC-3 are evenly distributed around the entire cortex of one-cell *cdc-37(RNAi)* embryos throughout the cell cycle beginning just after the completion of meiosis (Fig. 3D-I; Fig. 4, column 4; *n*=12; data not shown for PAR-1). The abundance of PAR-1 and PAR-2 at the cortex appears to be reduced relative to control embryos. The relative abundance of PAR-6 and PKC-3 does not appear to be affected, although PKC-3 levels are lower by western blot assays (see below). GFP::PAR-6 in control embryos enters the nucleus at nuclear envelope breakdown in 10 out of 10 embryos (not shown) (Cuenca et al., 2003). This fails to occur in eight out of nine *cdc-37(RNAi)* embryos, and these embryos consistently exhibit a mitosis-specific peri-centrosomal accumulation of GFP::PAR-6 that is never seen in control embryos (Fig. 4). Finally, whereas PAR-6 accumulates in cortical puncta in wild-type embryos (Hung and Kemphues, 1999), in *cdc-37(RNAi)* embryos it has a much smoother cortical distribution (data not shown).

Surprisingly, PAR-3 behaves differently from PAR-6 and PKC-3 in *cdc-37(RNAi)* embryos. In control embryos, PAR-3 is evenly distributed along the entire cortex early in the cell cycle and becomes restricted to the anterior of the cell along with PAR-6 and PKC-3 (Etemad-Moghadam et al., 1995) (Fig. 3B; Fig. 4; *n*=82). In *cdc-37(RNAi)* embryos, PAR-3, like PKC-3 and PAR-6, has a significant overlap with PAR-2 (Fig. 3D-F; *n*=57). However, in these embryos PAR-3 forms large cortical aggregates, and is more patchily distributed than are PAR-6 and PKC-3 (Fig. 3E,F; Fig. 4). Furthermore, unlike PAR-6 and PKC-3, which remain uniformly distributed around the cortex in *cdc-37(RNAi)* embryos, PAR-3 clears from the posterior cortex during pronuclear migration. In control embryos, PAR-3 clears from the posterior cortical region to 49%±5% of the total egg length (*n*=10); in *cdc-37(RNAi)* embryos, the maximal clearing reaches only 40%±11% (*n*=19) of the egg length. Finally, whereas PAR-6 and PKC-3 remain cortical throughout the cell cycle in *cdc-37(RNAi)* embryos, PAR-3 consistently disappears from the cortex at metaphase (Fig. 4, column 2, fourth image). PAR-3 returns to the cortex late in the cell cycle and is distributed to both daughter cells in a patchy and variable distribution, disappearing again at the next metaphase and coming back to the cortex late in the second cell cycle. This pattern of PAR-3 dynamics is similar to that observed in *par-6* mutant and *pkc-3(RNAi)* embryos (Tabuse et al., 1998; Watts et al., 1996).

These results were unexpected because in the *cdc-37(+)* background, cortical localization of PAR-6 and PKC-3 is dependent upon PAR-3 (Hung and Kemphues, 1999; Tabuse et al., 1998). Therefore, we hypothesized that CDC-37 activity contributes to the normal dynamics of these proteins at the cortex, but when it is reduced or absent PAR-6 and PKC-3 can accumulate at the cortex independently of PAR-3.

To test this hypothesis, we compared the distribution of PAR-6 and PKC-3 in *par-3(it71)* embryos with or without RNAi-mediated depletion of CDC-37 (Fig. 5). As previously reported (Hung and Kemphues, 1999; Tabuse et al., 1998) in *cdc-37(+)*; *par-3(it71)* embryos, PAR-6 and PKC-3 are not detectable at the cortex at any stage in the cell cycle (Fig. 5A,C; *n*=50). However, in *cdc-37(RNAi)*; *par-3(it71)* embryos, PAR-6 and PKC-3 accumulate at the cortex but are not asymmetrically localized (Fig. 5B,D; *n*=42). Thus, cortical accumulation of PAR-6 and PKC-3 is dependent upon PAR-3 only in the presence of normal levels of CDC-37.

To determine whether CDC-37 acts preferentially through PAR-6 or PKC-3, we depleted CDC-37 in *par-6(zu222)* worms (Fig. 5G), and doubly depleted PKC-3 and CDC-37 in wild-type worms (Fig. 5H), and assayed the remaining anterior complex proteins by immunofluorescence microscopy. As previously shown by Hung and Kemphues, in *par-6(zu222)* worms, PKC-3 is not detectable at the cortex (Hung and Kemphues, 1999) (Fig. 5G; *n*=21). PKC-3 is also absent from the cortex in *cdc-37(RNAi); par-6(zu222)* embryos at all stages of the first cell cycle (Fig. 5H; *n*=25). As shown by Tabuse and colleagues, in *pkc-3(RNAi)* embryos, PAR-6 is not detectable at the cortex (Tabuse et al., 1998) (Fig. 5E; *n*=102). However, after double RNAi of PKC-3 and CDC-37, PAR-6 is present symmetrically at the cortex of one-cell embryos at all stages of the first cell cycle (Fig. 5F; *n*=170). Thus, in a *cdc-37(RNAi)* background, PAR-6 is required for PKC-3 localization to the cortex, but PKC-3 is not required for PAR-6 cortical localization. We interpret these results to mean that CDC-37 is required to prevent PAR-6 from associating with the cortex, and that PAR-3 normally acts to block the action of CDC-37.

We also examined the distribution of PAR-3 in these doubly depleted embryos. We found, as expected, that PAR-3 becomes partially restricted to the anterior cortex in *par-6* mutant embryos, *pkc-3(RNAi)* embryos, *cdc-37(RNAi)* embryos, *pkc-3(RNAi); cdc-37(RNAi)* and *par-6(zu222); cdc-37(RNAi)* embryos (data not shown). However, we noted that removal of PAR-6 or depletion of PKC-3 in *cdc-37(RNAi)* embryos led to a slight increase in the levels of cortical PAR-3 (data not shown).

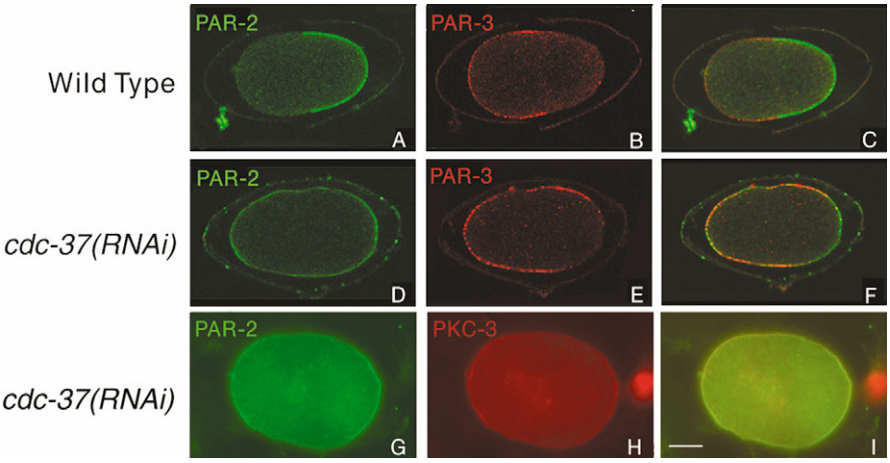

Fig. 3. PAR proteins are mislocalized in *cdc-37(RNAi)* embryos. (**A-F**) Confocal immunofluorescence images of late-prophase stage one-cell embryos showing distributions of PAR-3 (red) and PAR-2 (green) in wild-type (A-C) and *cdc-37(RNAi)* (D-F) embryos. (**G-I**) Wide-field immunofluorescence images of a *cdc-37(RNAi)* metaphase one-cell embryo showing the complete overlap of the PAR-2 (green) and PKC-3 (red) domains.

Cortical localization of PAR-6 in *cdc-37(RNAi)* embryos depends upon CDC-42

As described above, *cdc-37(RNAi)* allows constitutive cortical accumulation of PAR-6. If this reflects a role for CDC-37 in the normal mechanism for PAR-6 cortical accumulation and asymmetry, we would expect this cortical accumulation to be dependent upon the Rho-GTPase CDC-42. Binding to CDC-42 is required for the proper accumulation and maintenance of PAR-6 at the cortex of the one-cell embryo (Gotta et al., 2001; Kay and Hunter, 2001) (D. Aceto, M.B. and K.K., unpublished). In *cdc-37(RNAi)* embryos, GFP::PAR-6 is evenly distributed around the entire cortex (Fig. 4, column 4). By contrast, in *cdc-42(RNAi)* embryos, a reduced amount of GFP::PAR-6 accumulates at the cortex early in the first cell cycle and becomes partially restricted to the anterior, but is undetectable after metaphase (Fig. 6A,B; D. Aceto, M.B. and K.K., unpublished). We found that depleting both CDC-42 and CDC-37 by RNAi results in a phenotype that differs from either single RNAi. In *cdc-42(RNAi); cdc-37(RNAi)* embryos, GFP::PAR-6 does not accumulate at the cortex (7/11 embryos; Fig. 6C,D). Thus, CDC-42 is required for the constitutive cortical accumulation of PAR-6 in *cdc-37(RNAi)* embryos, and CDC-37 is required for the residual PAR-6 in *cdc-42(RNAi)* embryos.

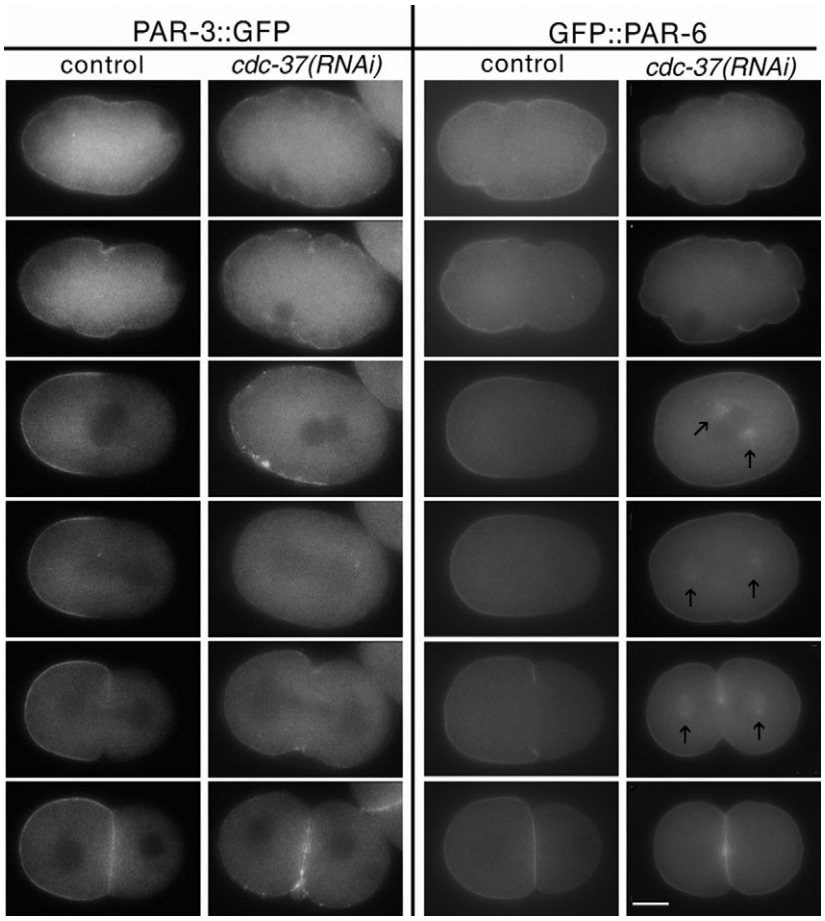

Fig. 4. Depletion of CDC-37 affects the distribution of PAR-3 and PAR-6 differently. Each column shows multiple images from a wide-field microscopy time-lapse movie of a single embryo through the first cell cycle. Note that, in control embryos, cortical PAR-3::GFP (column 1) and GFP::PAR-6 (column 3) are co-localized and asymmetric, whereas the two proteins behave differently in *cdc-37(RNAi)* embryos (columns 2 and 4; see Results). The arrows point to the pericentriolar accumulation of GFP::PAR-6 in the *cdc-37(RNAi)* embryos. Scale bar: ~10 μM.

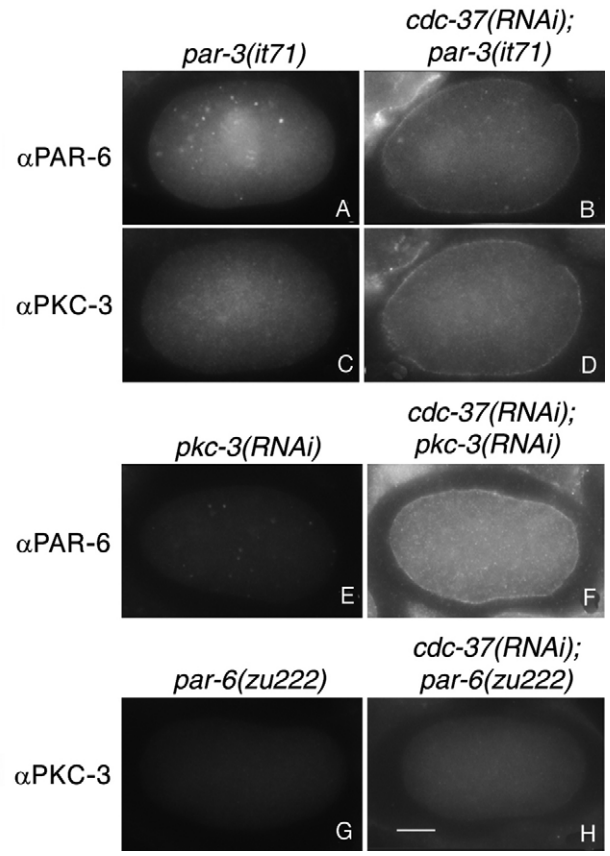

Fig. 5. Distributions of PAR-6 and PKC-3 after single and double depletions of CDC-37 and anterior PAR proteins. All embryos in the immunofluorescence images are at late prophase or metaphase of the first cell cycle. (**A-D**) PAR-6 distribution (A,B) and PKC-3 distribution (C,D) in *par-3(it71)* and *par-3(it71); cdc-37(RNAi)* treated embryos. (**E**,**F**) PAR-6 localization in the *pkc-3(RNAi)* or *pkc-3(RNAi); cdc-37(RNAi)* background. (**G**,**H**) PKC-3 localization in *par-6(zu222)* or *par-6(zu222); cdc-37(RNAi)* treated embryos. The cytoplasmic particles in A, B and E are P granules that are detected with some preparations of affinity-purified anti-PAR-6 antibody.

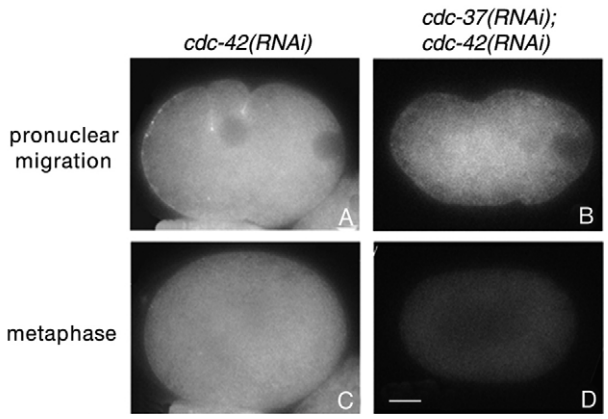

Fig. 6. PAR-6 protein does not accumulate at the cortex in *cdc-37(RNAi); cdc-42(RNAi)* embryos. (**A**,**C**) GFP::PAR-6 embryo treated with *cdc-42(RNAi)*. (A) Punctate GFP::PAR-6 becomes somewhat asymmetric early in the cell cycle. (C) At metaphase, GFP::PAR-6 becomes undetectable at the cortex. (**B**,**D**) GFP::PAR-6 embryos treated with *cdc-37(RNAi); cdc-42(RNAi)*. GFP::PAR-6 does not become cortical at any stage in the cell cycle. Control uninjected or *cdc-37(RNAi)* embryos treated on the same day looked the same as embryos in Fig. 4, columns 3 and 4, respectively.

The similarity between the behavior of PAR-3 in *cdc-37(RNAi)* and the residual PAR-6 in *cdc-42(RNAi)* led us to wonder whether most or all of the residual cortical PAR-6 in *cdc-42(RNAi)* embryos might be associated with PAR-3. To test this, we examined the extent of overlap of PAR-3 and PAR-6 in cortical puncta in *cdc-42(RNAi)* embryos (see Materials and methods). Cortical sampling of uninjected control GFP::PAR-6 embryos stained with antibodies specific to GFP and PAR-3 showed that 65% of the PAR-6 puncta overlap with PAR-3 in the wild type (Fig. 7A-C; see also Table S1 in the supplementary material). By contrast, cortical sampling in GFP::PAR-6 embryos treated with *cdc-42(RNAi)* showed that 90% of PAR-6 puncta overlap with PAR-3 (Fig. 7D-F; see Table S1 in the supplementary material). This extent of overlap is similar to that seen previously in control experiments using two different anti-PAR-3 antibodies (Hung and Kemphues, 1999), and thus is consistent with the hypothesis that most or even all cortical PAR-6 in *cdc-42(RNAi)* embryos is associated with PAR-3. The proportion of puncta that contained only PAR-3 did not show a statistically significant difference between control and *cdc-42(RNAi)* embryos (see Table S1 in the supplementary material). These results suggest that there are two sites for PAR-6 cortical association, one dependent on CDC-42, and the other independent of CDC-42 and colocalizing with PAR-3.

NMY-2::GFP distribution is altered in *cdc-37(RNAi)* embryos

CDC-37-depleted embryos exhibit altered cortical behaviors in the zygote. To understand the basis for this, we examined the distribution of NMY-2, the heavy chain of embryonic cytoplasmic myosin (Guo and Kemphues, 1996). Just after the completion of meiosis in wild-type embryos, NMY-2::GFP is found in distinct foci and filaments throughout the entire cortex. In response to the polarization signal, the cortical cytoskeleton, including the NMY-2::GFP foci, flows into the anterior (Munro et al., 2004). To determine the effect of knockdown of CDC-37 on NMY-2 localization, we examined *cdc-37(RNAi)* and control embryos expressing NMY-2::GFP. We found that, in *cdc-37(RNAi)* embryos, NMY-2::GFP forms foci and filaments like wild-type controls do. The foci flow into the anterior, clearing approximately 40% of the posterior cortex in contrast to the 50% clearing observed in control embryos. Based on descriptions by Munro and colleagues (Munro et al., 2004), this behaviour is similar to that seen when anterior PAR proteins are reduced or eliminated. As the two pronuclei migrate to the center of the embryos, the large NMY-2 foci in the anterior are replaced by fine fibers, as occurs in controls; however, in contrast to controls, asymmetry is lost. Cortical myosin drops to a level normally seen in the posterior (see Fig. S3 in the supplementary material).

CDC-37 protein is uniformly distributed in the cytoplasm and accumulates weakly on the spindle at mitosis

Previous work had shown that GFP::CDC-37 exhibited a distribution typical of free cytosolic proteins (Gunsalus et al., 2005). We independently constructed a GFP::CDC-37 translational fusion expressed under the control of the *pie-1* promoter and generated

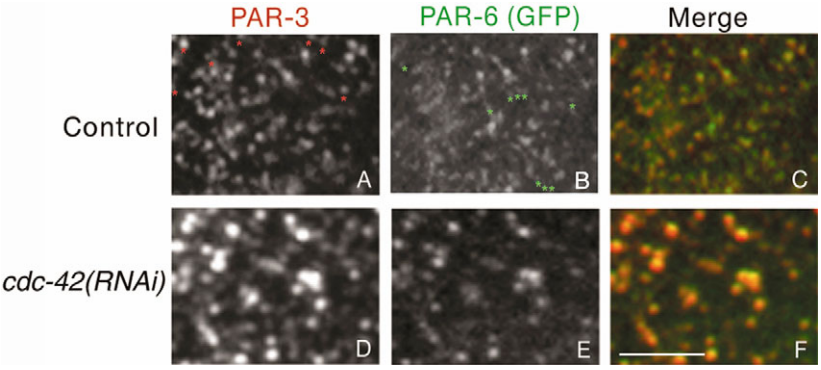

Fig. 7. PAR-6 puncta that do not contain PAR-3 are rare in *cdc-42(RNAi) embryos.* (**A-F**) Immunofluorescence images of anterior cortical patches of control embryos (A-C) or *cdc-42(RNAi)* embryos (D-F), showing the distributions of PAR-3 (red) and GFP::PAR-6 (green) puncta. In A, examples of puncta positive for only anti-PAR-3 are marked with red asterisks. In B, examples of puncta positive for only anti-GFP are marked with green asterisks. Note the larger puncta and the much more extensive overlap of anti-PAR-3 and anti-GFP positive puncta in D-F. Embryos examined were at late prophase of the first mitotic cell cycle.

transgenic lines by biolistic bombardment (Praitis et al., 2001). We recovered nine independent lines showing similar GFP expression in the embryo. The *Ppie-1::gfp::cdc-37* transgene suppresses the lethality of *cdc-37(RNAi)*, indicating that the transgene is functional (see Materials and methods). As previously reported, from meiosis until NEB, GFP::CDC-37 is evenly distributed throughout the cytoplasm in a pattern consistent with free cytosolic proteins (Fig. 8A-C). In our strains, at NEB, GFP::CDC-37 remains predominantly cytoplasmic but becomes transiently enriched around the chromosomes (Fig. 8D). As mitosis progresses, CDC-37 becomes slightly enriched on the spindle (Fig. 8E). Upon nuclear envelope reformation, CDC-37 is excluded from the nucleus (Fig. 8F).

cdc-37(RNAi) reduces steady-state levels of PKC-3 and a minor isoform of PAR-4

Because of the known role of CDC37 proteins as co-chaperones, we investigated whether CDC-37 depletion might influence the level of any of the PAR proteins in the early embryo. In two independent RNAi experiments, the steady state levels of PAR-1, PAR-3, PAR-5 and PAR-6 proteins were indistinguishable between control and *cdc-37(RNAi)* embryo extracts by western analysis.

PKC-3 and PAR-4 protein levels, however, were affected by *cdc-37(RNAi)*. PKC-3 levels were reduced in two out of three experiments by more than 80% (Fig. 9A). The effect on PAR-4 was less pronounced. When wild-type embryonic proteins were separated by gel electrophoresis and probed with a PAR-4 antibody, two predominant bands were observed: a faster migrating band representing about 90% of the antibody-reactive protein and a slower band (Fig. 9B). The slower migrating band is a phosphorylated form of the protein, as this band is eliminated by treatment of the sample with phosphatase (data not shown). Several independent samples of *cdc-37(RNAi)* embryos have shown a consistent reduction of the slower migrating PAR-4 band.

DISCUSSION

We have found that a homolog of yeast and vertebrate CDC37 proteins is required for embryonic polarity in *C. elegans*. Based on RNAi phenotypes, *C. elegans* CDC-37 is required for two major activities in the establishment of polarity. CDC-37 is required for the mutual exclusion of PAR-2 and the anterior PAR proteins, and for normal interactions among the anterior PAR proteins. We propose that the RNAi phenotypes arise in part because CDC-37 activity is

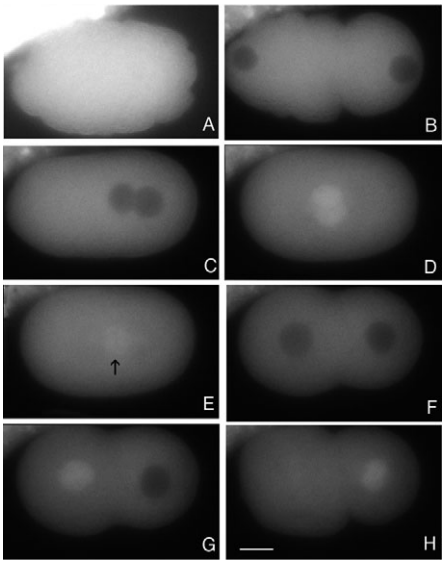

Fig. 8. GFP::CDC-37 is cytoplasmic with accumulation in the nucleoplasm and central spindle (marked by the arrow) during mitosis. Images are taken from a time-lapse movie of an embryo expressing GFP::CDC-37.

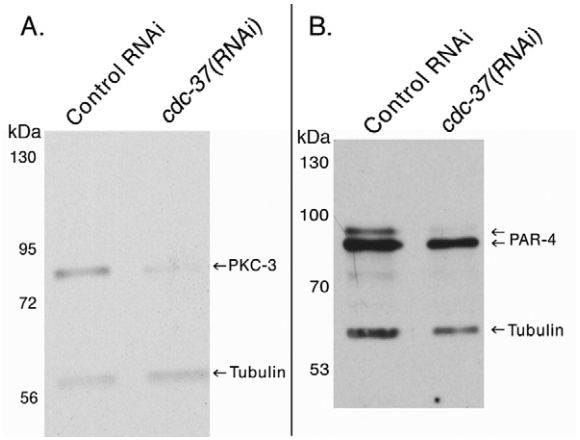

Fig. 9. PKC-3 and PAR-4 are affected by the depletion of CDC-37 by RNAi. (**A**,**B**) Western blots of protein extracts from embryos probed with either anti-PKC-3 antibody (A) or anti-PAR-4 antibody (B). Tubulin was used as a loading control. The upper arrow in B points to a phosphorylated form of PAR-4 that is also reduced in *cdc-37(RNAi)* embryos.

required to maintain PKC-3 levels, and in part because CDC-37 is required for the proper dynamic association of PAR-6 with two different cortical-binding sites.

Depletion of CDC-37 causes Par-like phenotypes

cdc-37(RNAi) embryos exhibit polarity-defective phenotypes, including altered cortical dynamics, equal first cleavage and failure to localize MEX-5 and P granules. These phenotypes apparently arise through the effect of CDC-37 on the distribution of the PAR proteins. It is probable that the embryonic phenotypes we describe do not represent the null condition, as at the time we sample embryos some CDC-37 protein remains.

Some *cdc-37(RNAi)* phenotypes can be explained by depletion of PKC-3

In wild-type embryos, stable cortical localization of the anterior PAR proteins, PAR-3, PAR-6 and PKC-3, requires the proper function of all three proteins (Hung and Kemphues, 1999; Tabuse et al., 1998; Watts et al., 1996). PAR-6 and PKC-3 are absolutely dependent upon PAR-3 (Hung and Kemphues, 1999; Tabuse et al., 1998), whereas PAR-3 exhibits only a partial dependence on the other two proteins. The reduced PAR-3 asymmetry, its patchy distribution and its disappearance at metaphase in *cdc-37(RNAi)* embryos is identical to what is observed in *par-6(zu222)* and *pkc-3(RNAi)* embryos (Tabuse et al., 1998; Watts et al., 1996). Indeed, PAR-3 distribution and dynamics are identical in *cdc-37(RNAi)* embryos, *par-6(zu222); cdc-37(RNAi)* embryos and *pkc-3(RNAi); cdc-37(RNAi)* embryos. A simple explanation for the effect on PAR-3 distribution and dynamics comes from the observation that PKC-3 levels are consistently reduced after *cdc-37(RNAi)* (see below). Reduced levels of PKC-3 can also account for the failure of PAR-2 to become restricted to the posterior, as exclusion of PAR-2 from the anterior requires the phosphorylation of PAR-2 by PKC-3 (Hao et al., 2006). Similar arguments may also hold for PAR-1 (Hao et al., 2006). NMY-2::GFP behaviour in *cdc-37(RNAi)* embryos can also be explained by reduced levels of PKC-3.

PAR-6 and PKC-3 cortical accumulation is independent of PAR-3 in *cdc-37(RNAi)* embryos

A reduction of PKC-3 cannot explain the entire *cdc-37(RNAi)* phenotype, however, as *pkc-3(RNAi)* and *cdc-37(RNAi)* phenotypes differ. In contrast to the failure of PAR-6 to accumulate cortically in *pkc-3(RNAi)* embryos (Tabuse et al., 1998), PAR-6 and the residual PKC-3 remain at the cortex throughout the cell cycle in *cdc-37(RNAi)* embryos, and do so even in the absence of PAR-3. Our epistasis analysis reveals that PAR-3-independent cortical localization of PKC-3 requires PAR-6, but that PAR-6 does not require PKC-3. Thus, reduction of CDC-37 renders PAR-6 and PKC-3 independent of PAR-3 for cortical localization, and renders PAR-6 independent of PKC-3 for its cortical localization.

We interpret these results to mean that CDC-37 activity normally influences the dynamics of the anterior complex proteins. We propose that CDC-37 and one or more of its client protein(s) function in wild-type cells to block the binding of PAR-6 to an unknown cortically associated protein. We further propose that binding to this cortical protein is part of the normal mechanism by which PAR-6 and PKC-3 localize to the anterior cortex. In wild-type cells, PAR-3 acts locally to antagonize the action of the CDC-37 client and allows PAR-6 to bind only in the anterior. In wild-type cells, this binding also requires PKC-3, perhaps because PAR-3 exerts its blocking effect via PKC-3.

PAR-6 requires CDC-42 to bind to the cortex in *cdc-37(RNAi)* embryos

It is also possible that the PAR-3-independent, cortical-binding site for PAR-6 in *cdc-37(RNAi)* embryos is spurious and has no normal role in anterior PAR protein function. Although we cannot rule this out, two observations make this unlikely. First, in keeping with previous immunolocalization results (Hung and Kemphues, 1999), we found that in wild-type embryos a substantial fraction of cortical PAR-6 does not colocalize in puncta with PAR-3. Second, the accumulation of PAR-6 at the cortex in *cdc-37(RNAi)* embryos is dependent upon CDC-42, just as it is in *cdc-37(+)* embryos. We also found that, in *cdc-42(RNAi)* embryos, all or most of the residual PAR-6-containing puncta also contain PAR-3. A further complexity of our results is that double depletion of CDC-37 and CDC-42 results in a complete absence of GFP::PAR-6 at the cortex, a phenotype that differs from that resulting from depletion of CDC-42 alone. This indicates that CDC-37 is required for the residual GFP::PAR-6 puncta in *cdc-42(RNAi)* embryos, suggesting that these puncta are not the result of partial depletion of CDC-42, but rather represent a different class of PAR-6-binding site.

We infer from these results that there are two different ways PAR-6 can localize to the cortex, and that both are mediated by CDC-37 (Fig. 10). The first mechanism is through *cdc-42*-independent binding to a PAR-3-containing complex, perhaps by direct binding to PAR-3. The second mechanism, mentioned above, is CDC-42 dependent, and is blocked by the action of CDC-37 and involves an unknown cortical-binding site. This site could be CDC-42 itself, or possibly a PDZ domain ligand whose binding to PAR-6 is regulated by CDC-42. This latter possibility is consistent with biochemical and structural studies of mammalian and fly PAR-6 proteins (Peterson et al., 2004). In these studies, the PAR-6 PDZ domain was found to be able to bind to a carboxy-terminal-type synthetic ligand in a CDC-42-regulated manner. PAR-6 was also found to bind weakly to the N-terminal PDZ domain of Bazooka (PAR-3) in a CDC-42-independent manner. Furthermore, the peptide ligand did not compete with PAR-3 for binding (Peterson et al., 2004). We also infer from our results and previously published results the existence of a class of PAR-3-containing

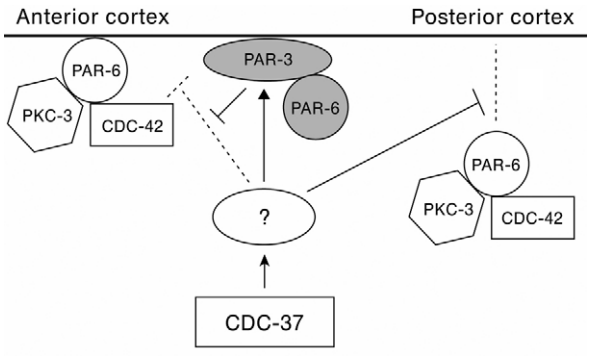

Fig. 10. Two possible modes of cortical association for PAR-6. Mode 1: (gray circle and oval) one or more CDC-37 clients (indicated by '?') are required for PAR-6 to bind to a PAR-3-containing complex, perhaps through direct binding to PAR-3, in a CDC-42-independent manner. Mode 2: (open shapes) one or more CDC-37 clients act to prevent CDC-42-dependent binding of PAR-6 at the cortex. PAR-3 or a protein regulated by PAR-3 acts locally to inhibit the action of the client protein, allowing CDC-42-dependent binding of PAR-6 only in the anterior.

puncta that do not contain PAR-6, and that in the early part of the cell cycle are independent of CDC-42, CDC-37, PKC-3 and PAR-6 for their cortical localization.

Our results contribute to a growing body of evidence that supports a dynamic regulation of anterior PAR protein distribution, as opposed to the simple concept of an obligate complex suggested by early biochemical and co-localization results. PAR-6 can bind to a variety of partners including Lethal Giant Larva (Betschinger et al., 2003; Plant et al., 2003; Yamanaka et al., 2003), Crumbs (Kempkens et al., 2006; Lemmers et al., 2004) and Pals1 (Hurd et al., 2003; Wang et al., 2004). Distinct distributions for Bazooka (PAR-3) versus PAR-6 and aPKC have been described in *Drosophila* epithelial cells and photoreceptors (Harris and Peifer, 2005; Nam and Choi, 2003), and Par3-independent cortical recruitment of Par6 and aPKC occurs in mammalian astrocytes (Etienne-Manneville and Hall, 2001). It will be interesting to learn to what extent the mechanisms for regulating these complexes are evolutionarily conserved.

cdc-37(RNAi) causes the depletion of the steady-state levels of PKC-3 and of phosphorylated PAR-4

CDC-37 is known to function as a protein chaperone in many systems, regulating the stability and function of many proteins, especially kinases (MacLean and Picard, 2003). We found that the steady-state level of PKC-3 is affected by depletion of CDC-37. Cdc37 was identified among proteins complexed with aPKC (Brajenovic et al., 2004), and thus may directly regulate its stability and, perhaps, its activity.

Biochemical support for our genetic evidence that another kinase (or kinases) might also be a client of CDC-37 comes from the observation that *cdc-37(RNAi)* consistently reduced the level of a phosphorylated form of PAR-4. The effect on this minor PAR-4 isoform, however, cannot account for all of the polarity phenotypes of the *cdc-37(RNAi)* embryos, because these phenotypes differ substantially from those of *par-4* loss-of-function mutants (Watts et al., 2000). We considered that PKC-3 might be functioning to phosphorylate PAR-4, but the phosphorylated form of PAR-4 was unaffected by *pkc-3(RNAi)* (M.B. and K.K., unpublished). We also considered the possibility that the unique *cdc-37(RNAi)* phenotype might be revealing a redundant function among the three known polarity kinases PAR-1, PAR-4 and PKC-3. However, doubly or triply depleted embryos (e.g. *par-4(it57); par-1(RNAi); pkc-3(RNAi)*) did not replicate the *cdc-37(RNAi)* phenotype (M.B. and K.K., unpublished). We also ruled out the possibility that the phenotype was a gain-of-function defect due to an imbalance between PAR-4 isoforms, by showing that *cdc-37(RNAi); par-4(it57)* embryos had early polarity defects identical to those of *cdc-37(RNAi)* alone (M.B. and K.K., unpublished).

We have shown that *C. elegans* CDC-37 has a role in the establishment of polarity in the one-cell embryo. We also present evidence that we interpret as indicating the existence of two modes of binding for PAR-6 at the cortex: CDC-42-dependent binding at a site that is normally blocked by the action of a CDC-37 client; and CDC-42-independent binding at a site that co-localizes with PAR-3 and that is also dependent upon a CDC-37 client. We propose that, in wild-type embryos, CDC-37-mediated inhibition of the CDC-42-dependent binding site and PAR-3-mediated release of this inhibition provide a key mechanism for the anterior accumulation of PAR-6. Identifying the ligand or ligands for cortical binding, and the relevant client or clients of CDC-37 that regulate this binding will advance our understanding of the mechanism of action of the anterior PAR proteins.

We thank Wendy Hoose and Mona Hassab for technical support, and Diane Morton, Kelly Liu and Sylvia Lee for helpful comments on the manuscript. We thank Didier Picard for yeast strains. M.B. was supported in part by NIGMS Predoctoral Training Grant GM007617. This work was funded by NICHD grant HD27689 and NIGMS grant GM079112 to K.K.

Supplementary material

Supplementary material for this article is available at http://dev.biologists.org/cgi/content/full/133/19/3745/DC1

References

Basso, A. D., Solit, D. B., Chiosis, G., Giri, B., Tsichlis, P. and Rosen, N. (2002). Akt forms an intracellular complex with heat shock protein 90 (Hsp90) and Cdc37 and is destabilized by inhibitors of Hsp90 function. *J. Biol. Chem.* **277**, 39858-39866.

Betschinger, J., Mechtler, K. and Knoblich, J. A. (2003). The Par complex directs asymmetric cell division by phosphorylating the cytoskeletal protein Lgl. *Nature* **422**, 326-330.

Boudeau, J., Deak, M., Lawlor, M. A., Morrice, N. A. and Alessi, D. R. (2003). Heat-shock protein 90 and Cdc37 interact with LKB1 and regulate its stability. *Biochem. J.* **370**, 849-857.

Boyd, L., Guo, S., Levitan, D., Stinchcomb, D. T. and Kemphues, K. J. (1996). PAR-2 is asymmetrically distributed and promotes association of P granules and PAR-1 with the cortex in *C. elegans* embryos. *Development* **122**, 3075-3084.

Bradford, M. M. (1976). A rapid and sensitive method for the quantitation of microgram quantities of protein utilizing the principle of protein-dye binding. *Anal. Biochem.* **72**, 248-254.

Brajenovic, M., Joberty, G., Kuster, B., Bouwmeester, T. and Drewes, G. (2004). Comprehensive proteomic analysis of human Par protein complexes reveals an interconnected protein network. *J. Biol. Chem.* **279**, 12804-12811.

Brenner, S. (1974). The genetics of *Caenorhabditis elegans*. *Genetics* **77**, 71-94.

Burnette, W. N. (1981). "Western blotting": electrophoretic transfer of proteins from sodium dodecyl sulfate–polyacrylamide gels to unmodified nitrocellulose and radiographic detection with antibody and radioiodinated protein A. *Anal. Biochem.* **112**, 195-203.

Cheeks, R. J., Canman, J. C., Gabriel, W. N., Meyer, N., Strome, S. and Goldstein, B. (2004). *C. elegans* PAR proteins function by mobilizing and stabilizing asymmetrically localized protein complexes. *Curr. Biol.* **14**, 851-862.

Cowan, C. R. and Hyman, A. A. (2004). Centrosomes direct cell polarity independently of microtubule assembly in *C. elegans* embryos. *Nature* **431**, 92-96.

Cuenca, A. A., Schetter, A., Aceto, D., Kemphues, K. and Seydoux, G. (2003). Polarization of the *C. elegans* zygote proceeds via distinct establishment and maintenance phases. *Development* **130**, 1255-1265.

Dai, K., Kobayashi, R. and Beach, D. (1996). Physical interaction of mammalian CDC37 with CDK4. *J. Biol. Chem.* **271**, 22030-22034.

Etemad-Moghadam, B., Guo, S. and Kemphues, K. J. (1995). Asymmetrically distributed PAR-3 protein contributes to cell polarity and spindle alignment in early *C. elegans* embryos. *Cell* **83**, 743-752.

Etienne-Manneville, S. and Hall, A. (2001). Integrin-mediated activation of Cdc42 controls cell polarity in migrating astrocytes through PKCzeta. *Cell* **106**, 489-498.

Fire, A., Xu, S., Montgomery, M. K., Kostas, S. A., Driver, S. E. and Mello, C. C. (1998). Potent and specific genetic interference by double-stranded RNA in *Caenorhabditis elegans*. *Nature* **391**, 806-811.

Gerber, M. R., Farrell, A., Deshaies, R. J., Herskowitz, I. and Morgan, D. O. (1995). Cdc37 is required for association of the protein kinase Cdc28 with G1 and mitotic cyclins. *Proc. Natl. Acad. Sci. USA* **92**, 4651-4655.

Gotta, M., Abraham, M. C. and Ahringer, J. (2001). CDC-42 controls early cell polarity and spindle orientation in *C. elegans*. *Curr. Biol.* **11**, 482-488.

Grammatikakis, N., Lin, J. H., Grammatikakis, A., Tsichlis, P. N. and Cochran, B. H. (1999). p50(cdc37) acting in concert with Hsp90 is required for Raf-1 function. *Mol. Cell. Biol.* **19**, 1661-1672.

Gunsalus, K. C., Ge, H., Schetter, A. J., Goldberg, D. S., Han, J. D., Hao, T., Berriz, G. F., Bertin, N., Huang, J., Chuang, L. S. et al. (2005). Predictive models of molecular machines involved in *Caenorhabditis elegans* early embryogenesis. *Nature* **436**, 861-865.

Guo, S. and Kemphues, K. J. (1995). *par-1*, a gene required for establishing polarity in *C. elegans* embryos, encodes a putative Ser/Thr kinase that is asymmetrically distributed. *Cell* **81**, 611-620.

Guo, S. and Kemphues, K. J. (1996). A non-muscle myosin required for embryonic polarity in Caenorhabditis elegans. *Nature* **382**, 455-458.

Hao, Y., Boyd, L. and Seydoux, G. (2006). Stabilization of cell polarity by the *C. elegans* RING protein PAR-2. *Dev. Cell* **10**, 199-208.

Harris, T. J. and Peifer, M. (2005). The positioning and segregation of apical cues during epithelial polarity establishment in Drosophila. *J. Cell Biol.* **170**, 813-823.

Hung, T. J. and Kemphues, K. J. (1999). PAR-6 is a conserved PDZ domain-containing protein that colocalizes with PAR-3 in *Caenorhabditis elegans* embryos. *Development* **126**, 127-135.

Hunter, T. and Poon, R. (1997). Cdc37: a protein kinase chaperone? *Trends Cell Biol.* **7**, 157-161.
Hurd, T. W., Gao, L., Roh, M. H., Macara, I. G. and Margolis, B. (2003). Direct interaction of two polarity complexes implicated in epithelial tight junction assembly. *Nat. Cell Biol.* **5**, 137-142.
Kay, A. J. and Hunter, C. P. (2001). CDC-42 regulates PAR protein localization and function to control cellular and embryonic polarity in *C. elegans*. *Curr. Biol.* **11**, 474-481.
Kemphues, K. J., Priess, J. R., Morton, D. G. and Cheng, N. S. (1988). Identification of genes required for cytoplasmic localization in early *C. elegans* embryos. *Cell* **52**, 311-320.
Kempkens, O., Medina, E., Fernandez-Ballester, G., Ozuyaman, S., Le Bivic, A., Serrano, L. and Knust, E. (2006). Computer modelling in combination with in vitro studies reveals similar binding affinities of Drosophila Crumbs for the PDZ domains of Stardust and DmPar-6. *Eur. J. Cell Biol.* **85**, 753-767.
Kirby, C., Kusch, M. and Kemphues, K. (1990). Mutations in the *par* genes of *Caenorhabditis elegans* affect cytoplasmic reorganization during the first cell cycle. *Dev. Biol.* **142**, 203-215.
Lemmers, C., Michel, D., Lane-Guermonprez, L., Delgrossi, M. H., Medina, E., Arsanto, J. P. and Le Bivic, A. (2004). CRB3 binds directly to Par6 and regulates the morphogenesis of the tight junctions in mammalian epithelial cells. *Mol. Biol. Cell* **15**, 1324-1333.
Li, S., Armstrong, C. M., Bertin, N., Ge, H., Milstein, S., Boxem, M., Vidalain, P. O., Han, J. D., Chesneau, A., Hao, T. et al. (2004). A map of the interactome network of the metazoan *C. elegans*. *Science* **303**, 540-543.
MacLean, M. and Picard, D. (2003). Cdc37 goes beyond Hsp90 and kinases. *Cell Stress Chaperones* **8**, 114-119.
Maduro, M. and Pilgrim, D. (1995). Identification and cloning of *unc-119*, a gene expressed in the *Caenorhabditis elegans* nervous system. *Genetics* **141**, 977-988.
McCarter, J., Bartlett, B., Dang, T. and Schedl, T. (1999). On the control of oocyte meiotic maturation and ovulation in *Caenorhabditis elegans*. *Dev. Biol.* **205**, 111-128.
Morton, D. G., Shakes, D. C., Nugent, S., Dichoso, D., Wang, W., Golden, A. and Kemphues, K. J. (2002). The *Caenorhabditis elegans par-5* gene encodes a 14-3-3 protein required for cellular asymmetry in the early embryo. *Dev. Biol.* **241**, 47-58.
Munro, E., Nance, J. and Priess, J. R. (2004). Cortical flows powered by asymmetrical contraction transport PAR proteins to establish and maintain anterior-posterior polarity in the early *C. elegans* embryo. *Dev. Cell* **7**, 413-424.
Nam, S. C. and Choi, K. W. (2003). Interaction of Par-6 and Crumbs complexes is essential for photoreceptor morphogenesis in Drosophila. *Development* **130**, 4363-4372.
Nance, J., Munro, E. M. and Priess, J. R. (2003). *C. elegans* PAR-3 and PAR-6 are required for apicobasal asymmetries associated with cell adhesion and gastrulation. *Development* **130**, 5339-5350.
Nishimura, T., Kato, K., Yamaguchi, T., Fukata, Y., Ohno, S. and Kaibuchi, K. (2004). Role of the PAR-3-KIF3 complex in the establishment of neuronal polarity. *Nat. Cell Biol.* **6**, 328-334.
Nony, P., Gaude, H., Rossel, M., Fournier, L., Rouault, J. P. and Billaud, M. (2003). Stability of the Peutz-Jeghers syndrome kinase LKB1 requires its binding to the molecular chaperones Hsp90/Cdc37. *Oncogene* **22**, 9165-9175.
Ohno, S. (2001). Intercellular junctions and cellular polarity: the PAR-aPKC complex, a conserved core cassette playing fundamental roles in cell polarity. *Curr. Opin. Cell Biol.* **13**, 641-648.
Parrish, S., Fleenor, J., Xu, S., Mello, C. and Fire, A. (2000). Functional anatomy of a dsRNA trigger: differential requirement for the two trigger strands in RNA interference. *Mol. Cell* **6**, 1077-1087.
Perdew, G. H., Wiegand, H., Vanden Heuvel, J. P., Mitchell, C. and Singh, S. S. (1997). A 50 kilodalton protein associated with raf and pp60(v-src) protein kinases is a mammalian homolog of the cell cycle control protein cdc37. *Biochemistry* **36**, 3600-3607.
Peterson, F. C., Penkert, R. R., Volkman, B. F. and Prehoda, K. E. (2004). Cdc42 regulates the Par-6 PDZ domain through an allosteric CRIB-PDZ transition. *Mol. Cell* **13**, 665-676.
Plant, P. J., Fawcett, J. P., Lin, D. C., Holdorf, A. D., Binns, K., Kulkarni, S. and Pawson, T. (2003). A polarity complex of mPar-6 and atypical PKC binds, phosphorylates and regulates mammalian Lgl. *Nat. Cell Biol.* **5**, 301-308.
Praitis, V., Casey, E., Collar, D. and Austin, J. (2001). Creation of low-copy integrated transgenic lines in *Caenorhabditis elegans*. *Genetics* **157**, 1217-1226.
Reed, S. I. (1980). The selection of *S. cerevisiae* mutants defective in the start event of cell division. *Genetics* **95**, 561-577.
Schubert, C. M., Lin, R., de Vries, C. J., Plasterk, R. H. and Priess, J. R. (2000). MEX-5 and MEX-6 function to establish soma/germline asymmetry in early *C. elegans* embryos. *Mol. Cell* **5**, 671-682.
Silverstein, A. M., Grammatikakis, N., Cochran, B. H., Chinkers, M. and Pratt, W. B. (1998). p50(cdc37) binds directly to the catalytic domain of Raf as well as to a site on hsp90 that is topologically adjacent to the tetratricopeptide repeat binding site. *J. Biol. Chem.* **273**, 20090-20095.
Sonnichsen, B., Koski, L. B., Walsh, A., Marschall, P., Neumann, B., Brehm, M., Alleaume, A. M., Artelt, J., Bettencourt, P., Cassin, E. et al. (2005). Full-genome RNAi profiling of early embryogenesis in Caenorhabditis elegans. *Nature* **434**, 462-469.
Stancato, L. F., Chow, Y. H., Hutchison, K. A., Perdew, G. H., Jove, R. and Pratt, W. B. (1993). Raf exists in a native heterocomplex with hsp90 and p50 that can be reconstituted in a cell-free system. *J. Biol. Chem.* **268**, 21711-21716.
Stepanova, L., Leng, X., Parker, S. B. and Harper, J. W. (1996). Mammalian p50Cdc37 is a protein kinase-targeting subunit of Hsp90 that binds and stabilizes Cdk4. *Genes Dev.* **10**, 1491-1502.
Strome, S. and Wood, W. B. (1982). Immunofluorescence visualization of germ-line-specific cytoplasmic granules in embryos, larvae, and adults of *Caenorhabditis elegans*. *Proc. Natl. Acad. Sci. USA* **79**, 1558-1562.
Strome, S. and Wood, W. B. (1983). Generation of asymmetry and segregation of germ-line granules in early *C. elegans* embryos. *Cell* **35**, 15-25.
Tabuse, Y., Izumi, Y., Piano, F., Kemphues, K. J., Miwa, J. and Ohno, S. (1998). Atypical protein kinase C cooperates with PAR-3 to establish embryonic polarity in *Caenorhabditis elegans*. *Development* **125**, 3607-3614.
Timmons, L. and Fire, A. (1998). Specific interference by ingested dsRNA. *Nature* **395**, 854.
Timmons, L., Court, D. L. and Fire, A. (2001). Ingestion of bacterially expressed dsRNAs can produce specific and potent genetic interference in *Caenorhabditis elegans*. *Gene* **263**, 103-112.
Wallenfang, M. R. and Seydoux, G. (2000). Polarization of the anterior-posterior axis of *C. elegans* is a microtubule-directed process. *Nature* **408**, 89-92.
Wang, Q., Hurd, T. W. and Margolis, B. (2004). Tight junction protein Par6 interacts with an evolutionarily conserved region in the amino terminus of PALS1/stardust. *J. Biol. Chem.* **279**, 30715-30721.
Watts, J. L., Etemad-Moghadam, B., Guo, S., Boyd, L., Draper, B. W., Mello, C. C., Priess, J. R. and Kemphues, K. J. (1996). *par-6*, a gene involved in the establishment of asymmetry in early *C. elegans* embryos, mediates the asymmetric localization of PAR-3. *Development* **122**, 3133-3140.
Watts, J. L., Morton, D. G., Bestman, J. and Kemphues, K. J. (2000). The C. elegans par-4 gene encodes a putative serine-threonine kinase required for establishing embryonic asymmetry. *Development* **127**, 1467-1475.
Wiggin, G. R., Fawcett, J. P. and Pawson, T. (2005). Polarity proteins in axon specification and synaptogenesis. *Dev. Cell* **8**, 803-816.
Yamanaka, T., Horikoshi, Y., Sugiyama, Y., Ishiyama, C., Suzuki, A., Hirose, T., Iwamatsu, A., Shinohara, A. and Ohno, S. (2003). Mammalian Lgl forms a protein complex with PAR-6 and aPKC independently of PAR-3 to regulate epithelial cell polarity. *Curr. Biol.* **13**, 734-743.